One-dimensional ordering in ferroelectric CsD_2PO_4 and CsH_2PO_4 as studied with neutron scattering

B. C. Frazer, D. Semmingsen,* W. D. Ellenson,† and G. Shirane
Brookhaven National Laboratory, Upton, New York 11973
(Received 19 April 1979)

The triple-axis neutron technique has been used in a detailed study of the intensity distribution and temperature dependence of the diffuse quasielastic scattering associated with the ferroelectric transitions in monoclinic CsD_2PO_4 and CsH_2PO_4. The diffuse scattering differs greatly from that observed previously in tetragonal KD_2PO_4, in which case the intensity distribution clearly exhibits characteristics of three-dimensional dipolar interactions. In the present study, the nature and extent of the diffuse scattering can be explained quantitatively on the basis of chainlike ordering with temperature-dependent interchain correlations. The variation in intensity measured perpendicular to the chains (which are parallel to the ferroelectric $\vec{b}$ axis) is mostly due to variations in the dynamical structure factor of a hydrogen-bonded chain of phosphate groups, and approaches a purely-one-dimensional form at temperatures well above T_c. The width of the scattering along the chain direction has been measured accurately for CsD_2PO_4 and yields an intrachain correlation of about 600 Å near T_c (264 K), decreasing to about 140 Å at 315 K. Near T_c, the cross section develops short-range three-dimensional interchain correlations with no appreciable change in linewidth. Very near T_c, the range of the latter is only about 30 Å.

I. INTRODUCTION

Hydrogen-bonded ferroelectrics have attracted considerable interest for some time from both theoretical and experimental points of view. In particular, numerous studies have been carried out on the tetragonal family of ferroelectric phosphates and arsenates, of which KH_2PO_4 (KDP) is the well-known prototype. As evident from the large effect deuteration has on the Curie temperatures in these crystals, the occurrence of ferroelectricity is in large degree associated with the hydrogen bonds in these materials.

The neutron scattering technique is particularly appropriate for the study of hydrogen-bond systems in crystals, but in only a few cases has it been used for detailed examinations of structural phase transitions in hydrogen-bonded ferroelectrics. Most of the information available has come from investigations of KD_2PO_4.[1,2] Studies on $ND_4D_2PO_4$,[3] and $H_2C_4O_4$ (squaric acid),[4] have provided some information on hydrogen-bonded antiferroelectrics for which sizable isotopic effects have also been observed, and a detailed study has been made on the very interesting case of copper formate tetrahydrate[5] in which ordering occurs in the water-molecule layers in this structure.

Ferroelectricity was reported[6] some time ago for CsH_2PO_4, even though this crystal does not belong to the tetragonal KDP family. The ferroelectric phase transition ($T_c = 154$ K) was confirmed recently by Levstik *et al.*[7] and by Uesu and Kobayashi.[8] The latter authors also carried out an x-ray structure analysis of the room-temperature paraelectric phase and established unambiguously that the true symmetry is monoclinic, space group $P2_1/m$ (C_{2h}^2), rather than orthohombic, as had been previously reported.[9] Levstik *et al.*[7] also carried out dielectric measurements on CsD_2PO_4 and found a large isotope effect [$T_c(D)/T_c(H) \sim 1.7$] since the ferroelectric transition was observed at 268 K. Therefore, as in the cases cited above, it is clear that collective behavior of protons (or deuterons) plays an essential role in this ferroelectric phase transition.

In all of these crystals where large isotope effects on T_c have been observed, one finds certain common features. The hydrogen bonds are short (~2.48–2.55 Å), although somewhat longer than "truly" symmetrical hydrogen bonds (~2.45 Å). Such bonds are expected to be of the double-well type, with a low intermediate barrier. Also, the hydrogen bonds link molecular-ionic groups (e.g., PO_4^{3-}), with very strong local interactions between the protons and the molecular electronic wave functions, and very-long-range correlations can easily develop in the networks formed by the hydrogen-bonded molecular-ionic groups. These correlations break the symmetry of the paraelectric phase locally above T_c in such a material, and when observable experimentally, indicate precursory development of the ferroelectric structure. In particular, they lead to temperature-dependent diffuse distributions of scattered neutron intensities, and this permits detailed

examination of a transition mechanism on a microscopic scale.

In a recent Letter,[10] we reported preliminary results of a neutron scattering study of the ferroelectric transition in CsD_2PO_4, with the conclusion that the diffuse scattering observed originates from chainlike ordering parallel to the ferroelectric b axis. The chains involved can be seen in the view of the isomorphous CsH_2PO_4 crystal structure provided in Fig. 1. The diffuse-scattering intensity distributions are quite different from those observed in the case of KD_2PO_4, as evident from the comparison shown in Fig. 2. The diffuse scattering from KD_2PO_4 clearly exhibits characteristics of correlations in a three-dimensional network, whereas that observed for CsD_2PO_4 is typical of a one-dimensional system.

In the present paper, we report the results of a more thorough study of this interesting material, based upon additional measurements on crystals of higher quality. The study was also extended to include measurements on CsH_2PO_4, although only limited data were collected in this case because of the high background from the hydrogen incoherent scattering. In addition to confirming the basic conclusions reached in an earlier paper, this more extensive study has provided a more accurate measure of the intrachain correlation length as a function of temperature, and has permitted development of a one-dimensional model in good agreement with experimental data.

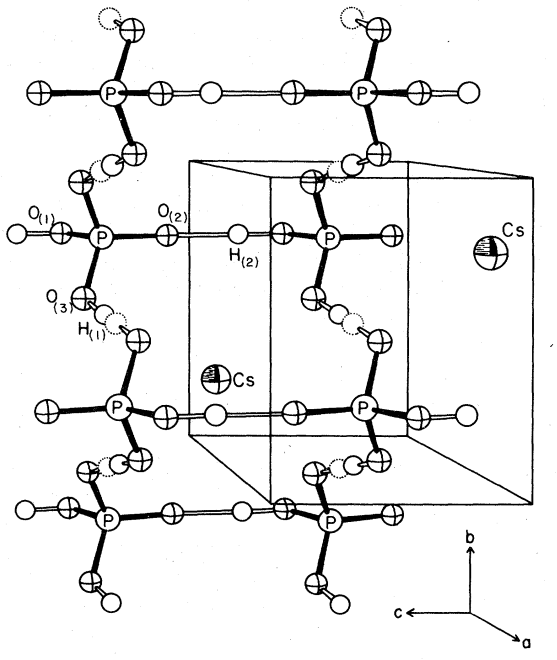

FIG. 1. Crystal structure of CsH_2PO_4. Disorder in the hydrogen bonds involved in chain formation is indicated by the neighboring closed and dotted circles used to represent the $H_{(1)}$ proton positions.

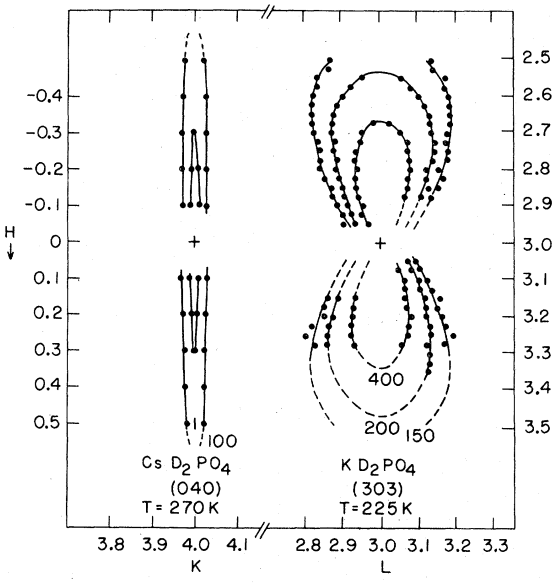

FIG. 2. Comparison of neutron diffuse-scattering intensity distributions for the paraelectric phases of CsD_2PO_4 and KD_2PO_4.

II. PRELIMINARY DETAILS

A. Crystal structure

Detailed crystal structure information is available from the x-ray structure analysis of the paraelectric phase of CsH_2PO_4 published by Uesu and Kobayashi,[8] and from the recent more extensive neutron diffraction studies of Semmingsen and Thomas[11] on the paraelectric and ferroelectric phases of both CsH_2PO_4 and CsD_2PO_4, and a similar study carried out by Nelmes and Choudhary[12] on CsH_2PO_4. We summarize here only some general features useful for the present paper.

CsH_2PO_4 and CsD_2PO_4 are strictly isomorphous in both phases. The basic structure consists of layers of hydrogen-bonded phosphate groups parallel with the crystallographic (100) planes, bonded together by Coulomb interactions with the Cs^+ ions. In contrast to the case of KH_2PO_4,[13] for which all hydrogen bonds are symmetry related, there are two crystallographically inequivalent hydrogen bonds in the structure. The shorter bond (2.48 Å) links the phosphate groups into the chains running along the unique b axis. The longer bond (2.54 Å), shown horizontal in Fig. 1, crosslinks the chains to form the (100) layers.

As inferred previously,[10] and since verified by the neutron structure analyses,[11,12] the longer bond is al-

ready ordered in the paraelectric phase, and its geometry is essentially unaltered on passing through the transition. The shorter bond is probably best described in terms of statistical distribution of the proton on two off-center equivalent sites above the transition, and an ordered asymmetric configuration below. In this proton ordering process, accompanied by other ionic displacements, the crystallographic center of inversion is lost and the $P2_1/m$ space group transforms to $P2_1$. There is no enlargement of the unit cell in this transformation, the number of molecules per unit cell remaining at 2.

B. Samples

CsH_2PO_4 can be prepared from stoichiometric amounts of $CsCO_3$ and aqueous H_3PO_4. After the carbon dioxide has been boiled off crystals of CsH_2PO_4 can then be grown from the solution. It was found, however, that a slight excess of H_3PO_4 is required in order to obtain good crystal growth. The pH of the starting solution thus prepared was about 2.5. Single crystals bounded by the forms {100} and {011} and of sizes up to about 1.5 g were then readily obtained. The deuterated material was prepared by several recrystallizations from D_2O with a stated purity of 99.7, the molar ratio between CsH_2PO_4 and D_2O each time being 1 to 8. The solution was also heated to boiling and then slowly evaporated to dryness to speed up exchange of hydrogen for deuterium. The final crystallization was carried out in a dessicator over anhydrous $CaSO_4$ (drierite). If complete exchange had been achieved the final deuterium content of the material should have been no less than 99%. However, the neutron structure analysis[11] of CsD_2PO_4 carried out at Brookhaven on a similarly prepared crystal leaves doubt as to the purity of the D_2O since refinement of the effective D scattering length gave a deuterium content of 94 ± 1%.

TABLE I. Monoclinic cell parameters in the paraelectric (P) and ferroelectric (F) phases of CsH_2PO_4 and CsD_2PO_4. Standard deviations are given in parentheses. T is the temperature at which measurements were made.

		T(K)	a(Å)	b(Å)	c(Å)	β
CsH_2PO_4	P	200	7.899(3)	6.325(3)	4.890(4)	108.29(3)
	F	100	7.899(3)	6.294(3)	4.898(2)	108.50(3)
CsD_2PO_4	P	298	7.918(2)	6.387(1)	4.885(1)	107.64(2)
	F	200	7.894(4)	6.327(3)	4.898(3)	107.95(4)

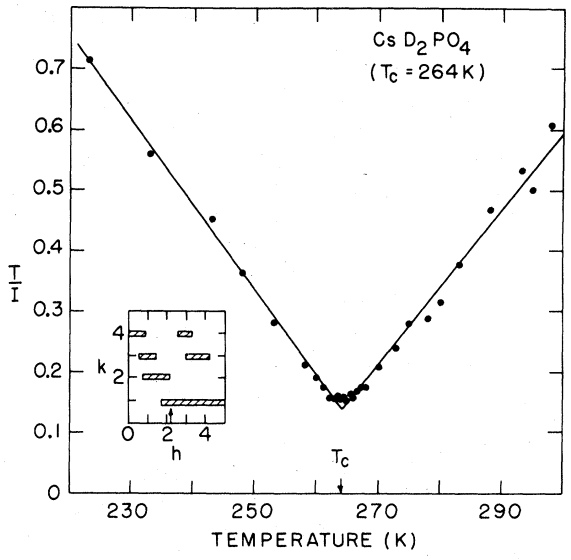

FIG. 3. Temperature dependence of inverse peak intensity (scaled by T) from $h = 2.15$ cross scans through the $k = 1$ diffuse scattering ridge, yielding $T_c = 264$ K for CsD_2PO_4. The shaded bars in the inset indicate the principal-diffuse-scattering regions in the ($hk0$) zone.

The samples were of good quality, giving a rocking curve with full width at half maximum (FWHM) of 0.18°. Lattice parameters of CsD_2PO_4 and CsH_2PO_4 were measured at $T \sim T_c \pm 50$ with results as given in Table I. The transition temperatures were determined from measurements of the temperature dependence of the diffuse scattering. This determination for CsD_2PO_4 is illustrated in Fig. 3. The T_c of 264 K is somewhat lower than that reported by Levstik *et al.*,[7] but assuming hydrogen contamination as discussed above, our results indicate a value of T_c close to 270 K for fully deuterated material. The measurements on CsH_2PO_4 yielded a transition temperature of 154.5 K, in moderately good agreement with that found by Levstik *et al.*

C. Instrumental

Measurements were carried out on triple-axis instruments at the high-flux beam reactor at Brookhaven National Laboratory. The monochromator was a curved pyrolytic graphite crystal with the (002) planes in reflecting position, and as the analyzer a planar pyrolytic graphite crystal was used, again with scattering from the (002) planes. For most measurements, the analyzer was set to the elastic position, which afforded a better signal-to-noise ratio in measurements of diffuse quasielastic scattering than could be obtained in a double-axis mode.

Two experimental configurations were employed.

Most of the measurements were made with a constant initial energy of 14.8 meV with higher-order contamination eliminated by use of pyrolytic graphite filters. The collimation was 20 min on each side of the sample and before the monochromator, and 40 min between the analyzer and detector (henceforth denoted 20-20-20-40). This configuration was used when high intensities were desired. For measurements where higher resolution was required the spectrometer was operated at 5.0 meV with a Be filter to avoid contamination. The collimation in this configuration was as before (20-20-20-40).

The samples were mounted on a cadmium covered aluminum pin and vacuum-sealed under He atmosphere in an aluminum can. The aluminum can was subsequently mounted in a cold gas-flow cryostat or in a closed cycle He refrigerator. Both instruments permit controlled temperature stabilization and regulation to 0.1 K can be obtained routinely.

III. NEUTRON SCATTERING MEASUREMENTS

Survey measurements at room temperature in the ($hk0$) zone of CsD_2PO_4 disclosed very narrow ridges of strong quasielastic diffuse scattering in several regions of reciprocal space (shown as shaded bars in the Fig. 3 inset). Measurements in the ($0kl$) zone, as well as tilting experiments out of the ($hk0$) zone, showed that the diffuse scattering is confined to planes, with k an integer, perpendicular to the b^* axis. No diffuse intensity was detectable in the ($h0l$) zone. These measurements were definitely indicative of a one-dimensional system, and a check on the temperature dependence of the diffuse scattering intensity established that this system is associated with the ferroelectric transition of the crystal.

Exploratory measurements were also made on low-frequency phonons propagating along a^* and b^*. Although acoustic branches were easily observable, no soft optic phonon could be found. Consequently, as in the case of KD_2PO_4, the transition does not result simply from an instability against a normal mode of vibration, but rather should be describable on an order-disorder model with proton (or deuteron) ordering mediated by damped proton-lattice interactions. Some significant differences from the KDP-type ferroelectrics can be expected, however, mainly because of the lower dimensionality but also from the absence of piezoelectricity (see, e.g., Takada *et al.*[14]; also see Cowley[15] on piezoelectric effects in KD_2PO_4 scattering data).

Following these initial surveys, detailed diffuse-scattering measurements were undertaken in the ($hk0$) zone of CsD_2PO_4. The open circle plots in Fig. 4 show the distributions of diffuse scattering observed in the ($hk0$) zone of CsD_2PO_4 as obtained scanning along the ridges at 280 K, a temperature

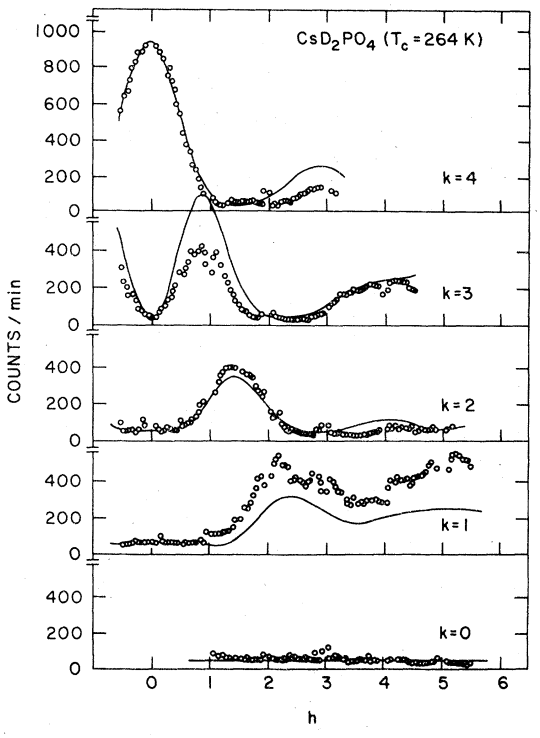

FIG. 4. Distribution of diffuse scatterring in the ($hk0$) zone of CsD_2PO_4 at $T = 280$ K measured in scans along h at constant values of k. Open circles represent experimental data and solid curves are from model calculations (discussed in Sec. IV).

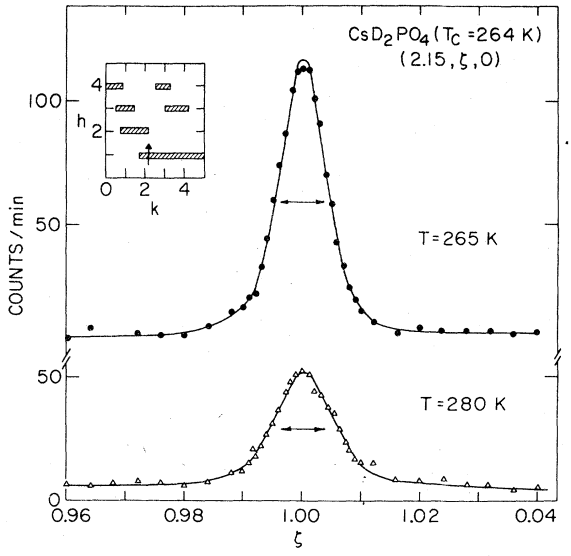

FIG. 5. High-resolution cross scans through the $k = 1$ ridge of CsD_2PO_4 at 265 K (just above T_c) and at 280 K. Incident-neutron energy of 5.0 meV. The double arrows at peak half maximum show instrumental resolution.

well above T_c. The sharply peaking contributions from Bragg scattering at the reciprocal-lattice points have been omitted. In all cases, the intensity varies rather slowly with h and, with the exception of (0,4,0), does not peak at reciprocal-lattice points.

In Fig. 5, we show a scan taken at the same temperature across the ridge, in the vicinity of the (2,1,0) reciprocal-lattice point, compared with a similar scan at 265 K, a temperature just above T_c. These particular scans were made using an incident neutron energy of 5 meV so as to obtain relatively high resolution. While the widths are quite narrow, they are clearly outside of instrumental resolution, and a significant narrowing is apparent at the lower temperature.

Detailed studies were carried out on the temperature dependence of the intensity distributions along the $(hk0)$ ridges. The results of scans along h at $k=1$ at four different temperatures are shown in Fig. 6. Here, as in Fig. 4, Bragg data points have been omitted. At temperatures close to the phase transition it is seen that the intensities peak up around the reciprocal-lattice points, indicating development of correlations between chains. At a temperature only 0.3 K above T_c, however, the intensity pattern is still quite diffuse, and not strongly suggestive of diverging three-dimensional critical scattering.

An interesting feature observed in the $(hk0)$ data is a dipping of the intensities near some reciprocal-lattice points. While not readily apparent in the data displayed in Figs. 4 and 6, this effect shows up clearly in the example given in Fig. 7 of high-resolution measurements of ridge intensities over a narrow range near (2,1,0), using a fine step interval of $\Delta h = 0.005$ with an incident neutron energy of 5.0 meV. These scans, along with similar measurements near other reciprocal-lattice points, established that the dips are not experimental artifacts, but instead represent a characteristic feature of this one-dimensional system.

Systematic diffuse scattering measurements were also made in the $(0kl)$ zone of CsD_2PO_4 and in the $(hk0)$ zone of CsH_2PO_4. Because of the relatively weak intensities and, in the case of CsH_2PO_4, the high incoherent scattering background from hydrogen, however, these measurements were not so extensive as those made for the $(hk0)$ zone of CsD_2PO_4. Careful survey measurements were made as well in the $(h0l)$ zone of CsD_2PO_4. In this latter case, as will come up later in connection with model

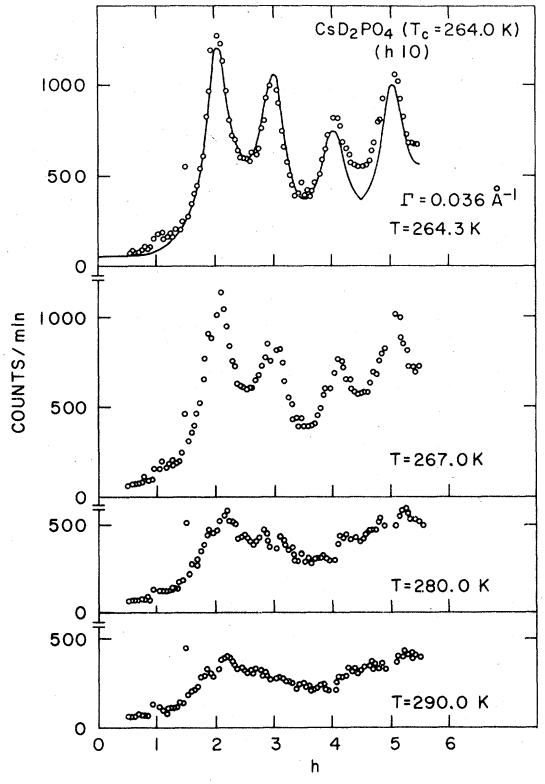

FIG. 6. Temperature dependence of the $k=1$ diffuse-scattering ridge in $(hk0)$ zone of CsD_2PO_4. The solid curve shown with the $T=264.3$ K data is from interchain correlation calculations (discussed in Sec. V).

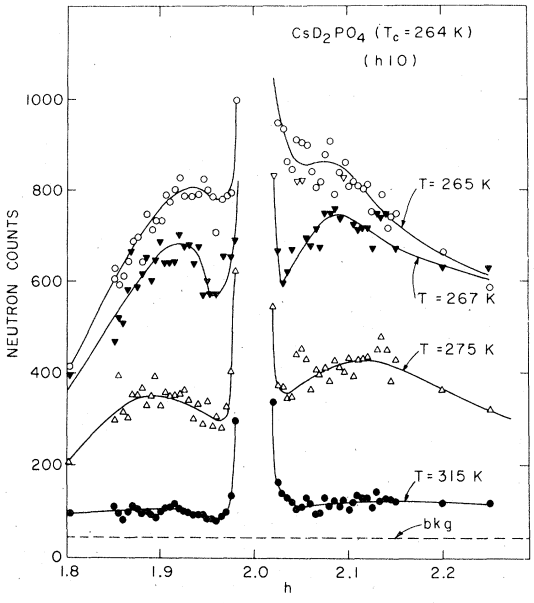

FIG. 7. High-resolution measurement at several temperatures of ridge intensities in vicinity of (210) in CsD_2PO_4, illustrating dips in diffuse scattering near reciprocal-lattice points. Incident neutron energy 5.0 meV. The resolution ellipsoid for these measurements had its major axis along h with FWHM of $0.012h$. The FWHM along k was $0.008k$.

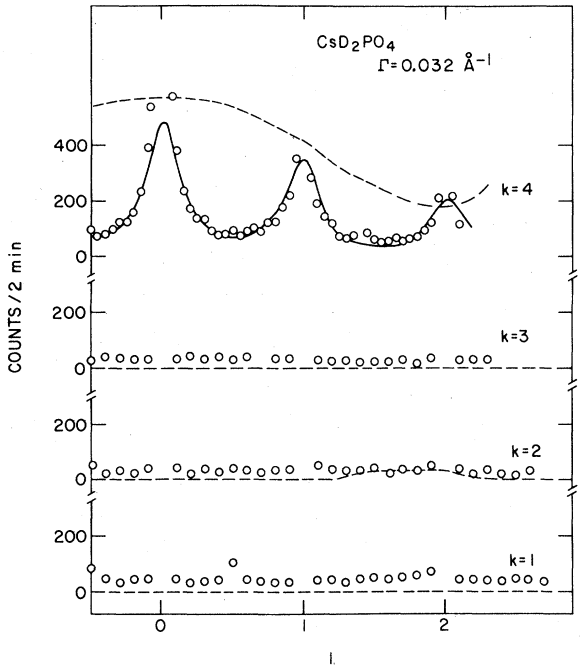

FIG. 8. Distribution of diffuse scattering in the $(0kl)$ zone of CsD_2PO_4 at 265 K (just above T_c). Open circles represent experimental data; dashed curves are from one-dimensional model calculations (see Sec. IV); and solid curve shown with $k=4$ data is from interchain correlation calculations (see Sec. V).

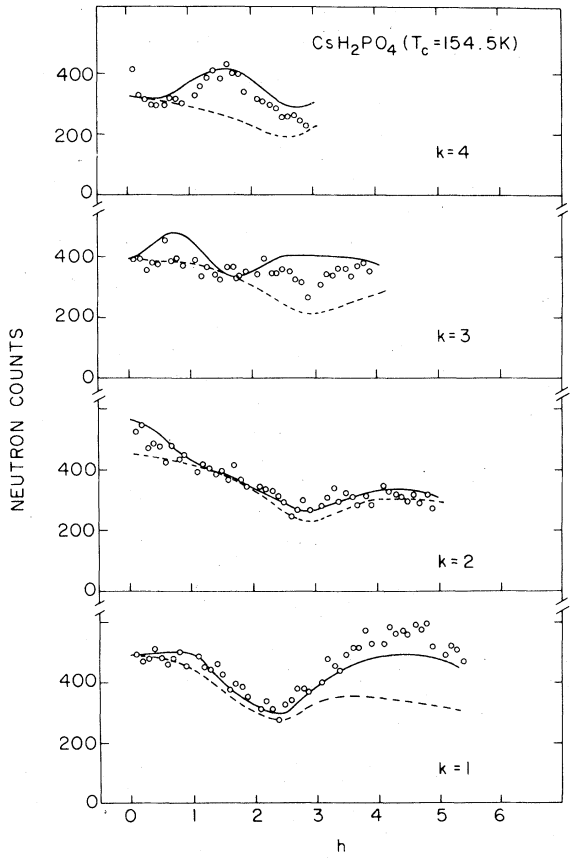

FIG. 9. Measurements (open circles) of diffuse scattering at 162 K in the $(hk0)$ zone of CsH_2PO_4. Solid curves are from one-dimensional model calculations (see Sec. IV), added to background (dashed curves).

calculations, no diffuse scattering related to the phase transition is to be expected, and indeed none was observed.

The diffuse scattering observable in the $(0kl)$ zone of CsD_2PO_4 is illustrated in Fig. 8. Readily measurable levels of intensity are largely confined to the ridge with $k=4$, at least within the range of $\vec{Q}$ for this study. The data shown were collected just above T_c where interchain correlations cause peaking near reciprocal-lattice points. Again, as in the $(hk0)$ case, the intensity pattern is still quite diffuse, and not indicative of incipient three-dimensional order. As the temperature is increased from T_c the changes in the intensity pattern are similar to those already noted for the $(hk0)$ case, except that notable peaking near reciprocal-lattice points persists to higher temperatures. The latter suggests that interchain correlations are somewhat stronger in the c direction than along a, although the overall behavior is still characteristic of a one-dimensional system.

Figure 9 shows data collected in the $(hk0)$ zone of CsH_2PO_4. The background, as indicated by the dashed curves in the figure, was quite high, but temperature-dependent ridges of diffuse scattering were clearly observable. The background curvature is due to the shape of the crystal, with higher apparent absorption, due to hydrogen scattering, for some scattering directions than for others. Background was measured by scanning parallel to the ridges. Cross scans through the ridges yielded very narrow curves, similar to those shown in Fig. 5 for CsD_2PO_4.

IV. MODEL CALCULATIONS

The diffuse-scattering cross section well above the transition may be described by the dynamical structure factor of the chain (for details relating generally to lower-dimensional systems see, e.g., J. W. Lynn *et al.*[16] and R. Pynn *et al.*[17])

$$F(\vec{Q}) = \sum_j b_j \exp(-W_j)(\vec{Q}\cdot\Delta\vec{r}_j)\exp(i\vec{Q}\cdot\vec{r}_j) \ , \qquad (1)$$

where the sum extends over all atoms in the unit cell, b_j is the scattering length of the jth atom, W_j is its Debye-Waller parameter, and $\Delta\vec{r}_j$ is its displacement from the crystallographic position $\vec{r}_j$ in the

TABLE II. Atomic coordinate parameters for CsD_2PO_4 in space group $P2_1/m$ and the displacement vectors associated with the transition to space group $P2_1$.

Atom type	Wyckoff set	$\vec{r}_j$	$\Delta\vec{r}_j$
$D_{(1)}$	a	$(0,0,0)$	$(\Delta x, \Delta y, \Delta z)$
		$(0,\frac{1}{2},0)$	$(\Delta\bar{x}, \Delta\bar{y}, \Delta\bar{z})$
$D_{(2)}$, $O_{(1)}$, $O_{(2)}$,	e	$(x,\frac{1}{4},z)$	$(0, \Delta y, 0)$
P, Cs		$(\bar{x},\frac{3}{4},\bar{z})$	$(0, \Delta y, 0)$
$O_{(3)}$	f	(x,y,z)	$(\Delta x, \Delta y, \Delta z)$
		$(\bar{x},\frac{1}{2}+y,\bar{z})$	$(\Delta\bar{x}, \Delta y, \Delta\bar{z})$
		$(x,\frac{1}{2}-y,z)$	$(\Delta\bar{x}, \Delta y, \Delta\bar{z})$
		$(\bar{x},\bar{y},\bar{z})$	$(\Delta x, \Delta y, \Delta z)$

TABLE III. Atomic displacement parameters for CsD_2PO_4.[a]

Atom α	Δx_α	Δy_α	Δz_α
$D_{(1)}$	0.0250	0.0205	−0.0002
$D_{(2)}$	0	0.0075	0
Cs	0	−0.0060	0
P	0	0.0165	0
$O_{(1)}$	0	0.0075	0
$O_{(2)}$	0	0.0075	0
$O_{(3)}$	0.0050	−0.0005	−0.0001

[a]Scale established by assuming a closest $D_{(1)}$-$O_{(3)}$ distance of 1.07 Å, as calculated from displaced positions. Relative error estimated at 0.0002 for Δx_α and Δz_α and at 0.0005 for Δy_α.

high-temperature structure. The displacement vectors $\Delta\vec{r}_j$ break the symmetry of the high-temperature phase but obey that of the low-temperature phase.

The atomic coordinate parameters for CsD_2PO_4 in the high-temperature space group $P2_1/m$ fall into three sets of equivalent positions, designated by a, e, and f in Wyckoff notation. These are listed in Table II along with the associated displacement vectors. The identifying subscripts for the oxygens are the same as those used by Uesu and Kobayashi.[8] $D_{(1)}$ refers to the deuterium involved in chain formation, and $D_{(2)}$ is ordered on the bonds shown horizontally in Fig. 1.

The structure factor expression (1) can be regarded as a sum of atomic structure factors

$$4\pi b_\alpha \exp(-W_\alpha)\phi_\alpha^{(\beta)} ,$$

where α refers to the atom type in Table III, and β identifies the Wyckoff set (a, e, or f). Each $\phi_\alpha^{(\beta)}$ contains a sum over all equivalent positions of atom α. For the $(hk0)$ zone, one then finds

$$\phi_{D_{(1)}}^{(a)} = \begin{cases} k\Delta y_{D_{(1)}}, & \text{for } k \text{ even} \\ h\Delta x_{D_{(1)}}, & \text{for } k \text{ odd} \end{cases} , \tag{2}$$

$$\phi_\alpha^{(e)} = \begin{cases} k\Delta y_\alpha \cos\dfrac{\pi k}{2}\cos 2\pi h x_\alpha, & \text{for } k \text{ even} \\ -k\Delta y_\alpha \sin\dfrac{\pi k}{2}\sin 2\pi h x_\alpha, & \text{for } k \text{ odd} \end{cases} , \tag{3}$$

$$\phi_{O_{(3)}}^{(f)} = \begin{cases} 2k\Delta y_{O_{(3)}}\cos 2\pi k y_{O_{(3)}}\cos 2\pi h x_{O_{(3)}} - 2h\Delta x_{O_{(3)}}\sin 2\pi k y_{O_{(3)}}\sin 2\pi h x_{O_{(3)}} , & \text{for } k \text{ even} \\ -2k\Delta y_{O_{(3)}}\sin 2\pi k y_{O_{(3)}}\sin 2\pi h x_{O_{(3)}} + 2h\Delta x_{O_{(3)}}\cos 2\pi k y_{O_{(3)}}\cos 2\pi h x_{O_{(3)}} , & \text{for } k \text{ odd} \end{cases} \tag{4}$$

Similar expressions hold for the $(0kl)$ zone if hx and $h\Delta x$ are replaced by lz and $l\Delta z$, respectively, and more generally for (hkl) if the replacement is by $(hx+lz)$ and $(h\Delta x + l\Delta z)$. We see that $\phi_\alpha^{(\beta)}$ is identically zero for all cases where $k=0$, in agreement with the absence of diffuse scattering in the $(h0l)$ zone (see, e.g., the $k=0$ plot in Fig. 4).

The diffuse-scattering intensity is proportional to $|F(Q)|^2$. The parameters varied in developing the refining models were the displacements $(\Delta x_\alpha, \Delta y_\alpha, \Delta z_\alpha)$ and a scale factor. The static coordinate parameters of all atoms except deuterium $D_{(1)}$, as well as the Debye-Waller parameters for all atoms, were taken from the crystal structure determinations—working initially with results of Uesu and Kobayashi[8] and turning later to the more complete information

available from the study of Semmingsen and Thomas.[11] The $D_{(1)}$ position was taken to be on the 2_1 axis at the midpoint of the O–D···O bond.

The values used for the scattering lengths (in units of 10^{-12} cm) were: $b_{Cs}=0.54$, $b_P=0.51$, $b_O=0.580$, $b_H=-0.374$, and $b_D=0.667$ (from the compilation of Dorner and Comès[18]). In late stages of the analysis a reduced effective value of 0.605 was used for b_D, for reasons alluded to in Sec. II B.

We see from Table II that there are eleven displacement parameters: three for $D_{(1)}$; one each for $D_{(2)}$, $O_{(1)}$, $O_{(2)}$, P, and Cs; and three for $O_{(3)}$. However, the requirement that the center of mass remain fixed reduces the number of parameters by one. The twofold symmetry automatically leaves the center of mass fixed for x and z displacements, but for y displacements we have the condition

$$\sum_j m_j \Delta y_j = 0 \ , \tag{5}$$

where m_j is the mass of atom j and the sum is taken over all atoms in the unit cell.

Calculations were carried out on a trial-and-error basis, starting in the $(hk0)$ zone of CsD_2PO_4 with some very simple chain models for which the PO_4 groups were assumed to move as rigid units, opposite to center of mass conserving Cs displacements. Initial trial values for the off bond center displacement components for $D_{(1)}$ in these models could be estimated fairly accurately from the extensive literature on hydrogen (and deuterium) bonds. The high intensity in the vicinity of (040) and near zero intensity for the case of (020) proved to be very useful in guiding early model development. (In these cases, the structure factors reduce to $\sum_j C_j \Delta y_j$, where the C_j's are constant coefficients.) Later, a generalized structure factor program, permitting variation of h over noninteger values at fixed integer values of k was used for rapid computer calculations to check trial models and to achieve improvements after an approximately correct model had emerged.

Although exhaustive refinement was not attempted, a model was found which gave remarkably good agreement with experimental data. The displacement parameters for this model are listed in Table III and its qualitative features are shown schematically in Fig. 10. Intensities calculated with these parameters are plotted as solid curves for comparison with experimental $(hk0)$ data in Fig. 4. A comparison with $(0kl)$ data is provided by the calculated dashed curves in Fig. 8, although in this case, where the observation temperature is very near T_c, and interchain correlations have developed, comparison of the one-dimensional calculation applies only to the observed diffuse peak heights. In agreement with experiment, the model yields appreciable intensity levels only for the $k=4$ ridge, and good matching is obtained there with peak heights. As shown in Fig. 9, this model also results in quite good agreement in a comparison of calculated and observed $(hk0)$ data for the hydrogeneous crystal, CsH_2PO_4.

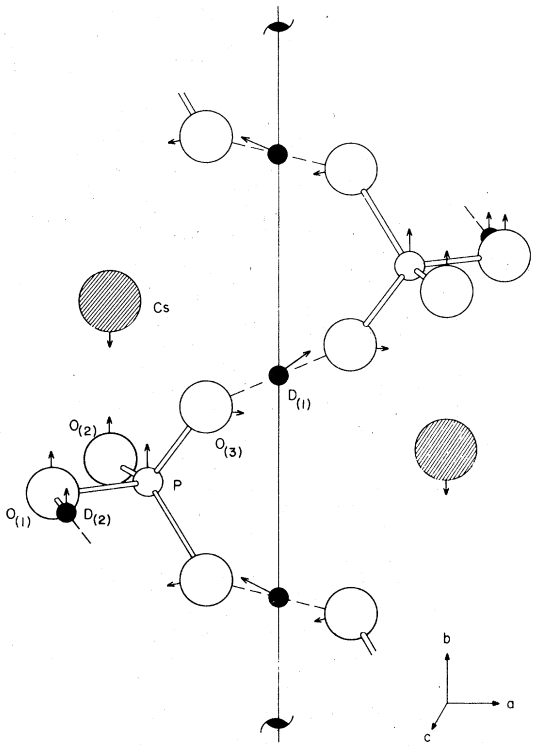

FIG. 10. Schematic representation of ferroelectric mode in CsD_2PO_4, as determined from model calculations discussed in Sec. IV. The twofold screw axis, shown parallel to the b axis, is the only symmetry element retained on passing through the phase transition.

V. INTRACHAIN AND INTERCHAIN CORRELATIONS

The cross scans shown in Fig. 5 provide representative plots of CsD_2PO_4 data for two of eight observation temperatures in the range 265 to 315 K, over which intrachain correlations were examined. As noted earlier, these scans were made under high-resolution conditions, using an incident neutron energy of 5 meV. It was possible to fit the experimental data quite accurately by folding a Lorentzian distribution, $I \propto 1/(q_\parallel^2+\Gamma^2)$, with the instrumental resolution, which was taken to be Gaussian. In this expression, $q_\parallel$ is measured parallel to the chain axis, or perpendicular to the ridge, and Γ, the HWHM (half width at half maximum) for the distribution, is the inverse correlation range in Å^{-1} along the chains. The solid curves in Fig. 5 show the calculated fits obtained at 280 and 265 K (just one degree above T_c).

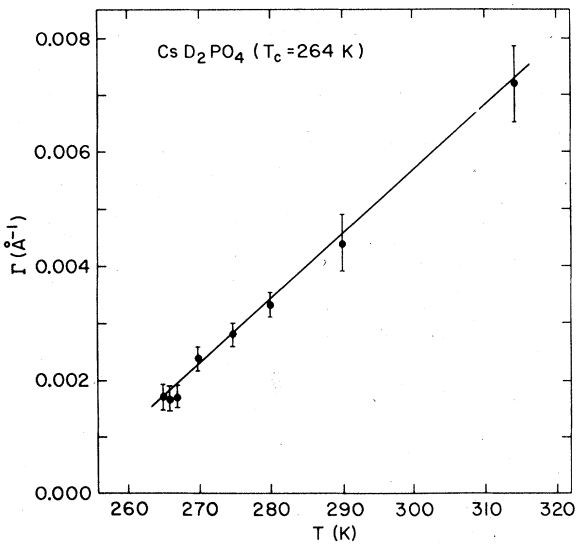

FIG. 11. Temperature dependence of CsD_2PO_4 intrachain inverse correlation range, Γ, as determined from neutron scattering measurements in $(hk0)$ zone.

The Γ values obtained over the experimental temperature range are plotted in Fig. 11. Close to T_c, the correlation range extends to almost 600 Å, or more than 180 PO_4 groups. At the highest temperature of measurement, about 50 K above T_c, the correlation range has dropped considerably, although it still extends to about 140 Å, or between 40 and 50 PO_4 groups. We also note that the intrachain correlation does not fully diverge at T_c.

Extraction of the interchain correlations, while similar in principle to the intrachain case, is complicated somewhat by the intensity modulations arising from the one-dimensional structure factor. As shown by the $(hl0)$ data displayed in Fig. 6, for example, the broad peaks which build up around reciprocal-lattice points appear to be approximately Lorentzian, but tails of the distributions from neighboring peaks overlap. Width contributions due to instrumental resolution are essentially negligible, but in fitting a Lorentzian of the form $I \propto 1/(q_\perp^2 + \Gamma^2)$, where $q_\perp$ is measured perpendicular to the chains, one must fold in the highly $q_\perp$ dependent contributions from the one-dimensional structure factor.

The fit obtained for measurements in the $(hk0)$ zone of CsD_2PO_4 is illustrated by the solid curve drawn with the 264.3 K data in Fig. 6. This yields an interchain correlation range along the a axis of only about 30 Å at a temperature just 0.3 K above T_c. This corresponds to about $3\frac{1}{2}$ chains. As the temperature is raised, the scattering rapidly approaches the limiting intensity distribution expected for completely uncorrelated chains.

The solid curve in Fig. 8 is the result of a similar fitting calculation in the $(0kl)$ zone. This indicates that the interchain correlation range along the c axis is also about 30 Å near T_c. Because of the chain arrangement in the structure, however, this corresponds to about $6\frac{1}{2}$ chains. This indication of somewhat stronger coupling along c, which is consistent with the observation noted earlier on the slower fall off with temperature of peaking at reciprocal-lattice points, is not very surprising when one considers the layerlike structure of the crystal and the sharing of Cs ions by neighboring chains.

VI. CONCLUDING REMARKS

The results reported here conclusively establish the basic one-dimensional nature of ordering in CsD_2PO_4 and its hydrogenous isomorph, CsH_2PO_4. As in the recently discussed case of $PbHPO_4$,[19] these materials provide a simple hydrogen-bonded system apparently well suited for description on a one-dimensional Ising model. They are also of particular interest in another aspect, since a paraelectric-ferroelectric-antiferroelectric triple point has been found[20] to occur in CsH_2PO_4 at a pressure of only 3.3 kbar and at a temperature of 135 K. CsD_2PO_4 exhibits similar behavior at somewhat higher pressure (~6 kbar).[21] A neutron scattering study of the high-pressure phase transition has been undertaken at Brookhaven, and the results will appear in a separate paper.[22]

The displacement of principal interest in the chain ordering mode discussed in Sec. IV, of course, is that of $D_{(1)}$ in the $O_{(3)} \cdots D_{(1)}-O'_{(3)}$ bond system. To first approximation, the mode can be considered otherwise in terms of rigid-body displacement of the PO_4 groups along the b axis, in opposition to the Cs ions. On closer inspection we see that there is an appreciable displacement of P relative to its surrounding $O_{(4)}$ tetrahedron, analogous to what has been observed in the KDP system.[2,13] In the latter case, significant differences were found in the P-O interatomic distances, depending on the oxygen association of hydrogen (or deuterium) in the ordering process.

In the present case, we should expect little or no change in the P-$O_{(1)}$ and P-$O_{(2)}$ distances, since $O_{(1)}$ and $O_{(2)}$ are involved with the already ordered $D_{(2)}$ bond system. This is borne out in a comparison of distances calculated on the one hand from crystallographic positions[11] in the paraelectric phase and on the other after applying the Table III displacements; in both cases $d_{P\text{-}O_{(1)}} = 1.57$ Å and $d_{P\text{-}O_{(2)}} = 1.49$ Å (where the close association of $D_{(2)}$ is with $O_{(1)}$). The two P-$O_{(3)}$ bonds, being crystallographically equivalent, yield a length of 1.53 Å in a calculation from structural data, but become unequal in the displaced calculation: $d_{P\text{-}O'_{(3)}} = 1.61$ Å and $d_{P\text{-}O_{(3)}} = 1.47$ Å (where $O'_{(3)}$ designates the oxygen with which $D_{(1)}$

becomes associated). We note the correspondence between the P-O cases for which there is close deuterium association (P-$O_{(1)}$ and P-$O'_{(3)}$) and between those where there is not (P-$O_{(2)}$ and P-$O_{(3)}$).

These comparisons are of some interest with regard to the reasonableness of the model, although the lengths of the displaced bonds are not considered to be highly accurate. Apart from the room for some further refinement in relative displacements in the model, the scaling assumption noted with Table III (taken from O-H distance results for KDP)[13] could also be subject to some trim up.

Finally, the observation of systematic dipping of intensities near reciprocal-lattice points (as illustrated in Fig. 7) is an interesting result of the present study, but the reason for the dips and their significance to the physics of this system are still under investigation as part of the continuing work at Brookhaven on CsD_2PO_4.[22]

ACKNOWLEDGMENTS

The authors are indebted to R. Youngblood and V. J. Emery for stimulating discussions and helpful suggestions. Research was supported by the Division of Basic Energy Sciences, DOE, under Contract No. EY-76-C-02-0016.

---

*Visiting scientist from the Univ. of Oslo, Oslo, Norway; now at Institutt for Atomenergi, Research Establishment Kjeller, 2007 Kjeller, Norway.

†Present address: Dept. of Chem., Univ. of Maine, Orono, Maine 04473.

[1]G. L. Paul, W. Cochran, W. J. L. Buyers, and R. A. Cowley, Phys. Rev. B 2, 4603 (1970).

[2]J. Skalyo, Jr., B. C. Frazer, and G. Shirane, Phys. Rev. B 1, 278 (1970).

[3]H. Meister, J. Skalyo, Jr., B. C. Frazer, and G. Shirane, Phys. Rev. 184, 550 (1969).

[4]E. J. Samuelsen and D. Semmingsen, J. Phys. Chem. Solids 38, 1275 (1977).

[5]R. Youngblood and J. D. Axe, Ferroelectrics 17, 435 (1977); R. Youngblood and J. D. Axe, Phys. Rev. B 17, 3639 (1978).

[6]F. Seidl, Tschermaks Mineral. Petrogr. Mitt. 1, 432 (1950).

[7]A. Levstik, R. Blinc, P. Kadaba, S. Cizikov, I. Levstik, and C. Filipic, Solid State Commun. 16, 1339 (1975).

[8]Y. Uesu and J. Kobayashi, Phys. Status Solidi A 34, 475 (1976).

[9]H. Fellner-Feldegg, Tschermaks Mineral. Petrogr. Mitt. 3, 37 (1952).

[10]D. Semmingsen, W. D. Ellenson, B. C. Frazer, and G. Shirane, Phys. Rev. Lett. 38, 1299 (1977).

[11]D. Semmingsen and R. Thomas (unpublished).

[12]R. J. Nelmes and R. N. P. Choudhary, Proceedings of the Fourth European Meeting of Crystallography, Oxford, England (1977) (unpublished); Solid State Commun. 26, 832 (1978).

[13]G. E. Bacon and R. S. Pease, Proc. R. Soc. London Sect. A 220, 397 (1953); A 230, 359 (1955).

[14]S. Takada, I. Ohnari, H. Kurosawa, and Y. Ohmura, Progr. Theor. Phys. 53, 936 (1975).

[15]R. A. Cowley, Phys. Rev. Lett. 36, 744 (1976).

[16]J. W. Lynn, M. Iizumi, G. Shirane, S. A. Werner, and R. B. Saillant, Phys. Rev. B 12, 1154 (1975).

[17]R. Pynn, J. D. Axe, and P. M. Raccah, Phys. Rev. B 17, 2196 (1978).

[18]B. Dorner and R. Comès, in *Dynamics of Solids and Liquids by Neutron Scattering, Topics in Current Physics,* edited by S. W. Lovesey and T. Springer (Springer, New York, 1977), Vol. 3, p. 136.

[19]A. V. de Carvalho and S. R. Salinas, J. Phys. Soc. Jpn. 44, 238 (1978).

[20]N. Yasuda, M. Okamoto, H. Shimuzu, S. Fujimoto, K. Yoshino, and Y. Inuishi, Phys. Rev. Lett. 41, 1311 (1978).

[21]K. Gesi and K. Ozawa, Jpn. J. Appl. Phys. 17, 435 (1978).

[22]R. Youngblood, J. Eckert, B. C. Frazer, and G. Shirane (unpublished).